Somatostatin secretion by Na^+-dependent Ca^{2+}-induced Ca^{2+} release in pancreatic delta-cells

Elisa Vergari[1,*], Geoffrey Denwood[1,*], Albert Salehi[3,4,*], Quan Zhang[1,*], Julie Adam[2], Ahmed Alrifaiy[3], Ingrid Wernstedt Asterholm[3,] Anna Benrick[3], Margarita V. Chibalina[1], Lena Eliasson[4], Claudia Guida[1], Thomas G. Hill[1], Alex Hamilton[1,4], Reshma Ramracheya[1], Frank Reimann[5], Nils J. G. Rorsman[1], Ioannis Spilliotis[1,6], Andrei I. Tarasov[1,6], Jonathan N. Walker[1], Patrik Rorsman[1,2,6,†] and Linford J. B. Briant[1,7,†]

[1]Oxford Centre for Diabetes, Endocrinology and Metabolism, Radcliffe Department of Medicine, Churchill Hospital, Oxford OX3 7LE, UK

[2]Nuffield Department of Clinical Medicine, University of Oxford, NDM Research Building, Oxford OX3 7FZ, UK

[3]Department of Neuroscience and Physiology, University of Göteborg, Box 430, SE40530 Göteborg, Sweden

[4]Department of Clinical Sciences Malmö, Clinical Research Centre, Box 50332, SE20213 Malmö, Sweden.

[5]MRC Metabolic Diseases Unit, University of Cambridge Metabolic Research Laboratories, WT-MRC Institute of Metabolic Science, University of Cambridge, Cambridge CB2 OQQ, UK

[6]Oxford National Institute for Health Research, Biomedical Research Centre, Churchill Hospital, Oxford OX3 7LE, UK

[7]Department of Computer Science, University of Oxford, Oxford OX1 3QD, UK

*Equal contribution.

†Address correspondence to Dr Linford Briant (linford.briant@ocdem.ox.ac.uk) or Professor Patrik Rorsman (patrik.rorsman@gu.se).

Pancreatic islets are complex micro-organs consisting of at least three different cell types: glucagon-secreting α-, insulin-producing β- and somatostatin-releasing δ-cells[1]. Somatostatin is a powerful paracrine inhibitor of insulin and glucagon secretion[2]. In diabetes, increased somatostatinergic signalling leads to defective counter-regulatory glucagon secretion[3]. This increases the risk of severe hypoglycaemia, a dangerous complication of insulin therapy[4]. The regulation of somatostatin secretion involves both intrinsic and paracrine mechanisms[5] but their relative contributions and whether they interact remains unclear. Here we show that dapagliflozin-sensitive glucose- and insulin-dependent sodium uptake stimulates somatostatin secretion by elevating the cytoplasmic Na^+ concentration ($[Na^+]_i$) and promoting intracellular Ca^{2+}-induced Ca^{2+} release (CICR). This mechanism also becomes activated when $[Na^+]_i$ is elevated following the inhibition of the plasmalemmal Na^+-K^+ pump by reductions of the extracellular K^+ concentration emulating those produced by exogenous insulin *in vivo*[6]. Islets from some donors with type-2 diabetes hypersecrete somatostatin, leading to suppression of glucagon secretion that can be alleviated by a somatostatin receptor antagonist. Our data highlight the role of Na^+ as an intracellular second messenger, illustrate the significance of the intraislet paracrine network and provide a mechanistic framework for pharmacological correction of the hormone secretion defects associated with diabetes that selectively target the δ-cells.

(200 words/200 allowed)

Somatostatin secretion from pancreatic δ-cells is a Ca^{2+}-dependent process involving influx of extracellular Ca^{2+} and mobilization of intracellular Ca^{2+} [5]. Mechanistic studies of the metabolic regulation of somatostatin secretion are complicated by the scarcity of δ-cells within the pancreatic islets (approx. 5%)[1]. To study the role of intracellular Ca^{2+} in the

regulation of somatostatin (Sst) secretion from δ-cells, we used mice expressing the genetically encoded Ca^{2+} sensor GCaMP3 in Sst-expressing cells (Sst-Cre-GCaMP3 mice[7]). These mice exhibited normal gross characteristics, glucose homeostasis and pancreatic islet hormone release (**Supplementary Fig. 1a-f**). Expression of GCaMP3 was confined to the δ-cells (**Supplementary Fig. 2a-c**). GCaMP3-positive cells had high expression of key δ-cell genes such as the intracellular Ca^{2+} release channels RyR3 and $InsP_3$ as well as the plasmalemmal voltage-gated R- and T-type Ca^{2+} channels (**Supplementary Table 1**). Of the glucose transporters, δ-cells expressed particularly high levels of *Glut1* but low expression of *Sglt1* and *Sglt2* was also detected.

We correlated Sst release and δ-cell cytoplasmic Ca^{2+} ($[Ca^{2+}]_i$) in Sst-Cre-GCaMP3 islets. Three examples of recordings of $[Ca^{2+}]_i$ in individual δ-cells within intact pancreatic islets are shown in **Fig. 1a**. The glucose responsiveness was variable: spontaneous $[Ca^{2+}]_i$ oscillations were observed in 27±3% of the cells at 1 mM glucose, which increased to 48±7% ($p<0.05$ vs 1 mM) at 4 mM and 82±5% at 20 mM glucose ($p<0.001$ vs 1 mM; 79 cells in 7 islets from 7 mice). Increasing glucose from 1 to 4 and 20 mM stimulated Sst release by 100% and 1000%, respectively (**Fig. 1b**), responses that were associated with comparable increases in the frequency of the $[Ca^{2+}]_i$ oscillations (**Fig. 1c**). When applied at 1 mM glucose, the K_{ATP} channel blocker tolbutamide (0.2 mM) produced a 5-fold increase in the frequency of the $[Ca^{2+}]_i$ oscillations (**Fig. 1d** and **Supplementary Fig. 3a**). Conversely, the K_{ATP} channel activator diazoxide and the L- and R-type Ca^{2+} channel blockers isradipine and SNX-482, respectively, abolished or reduced glucose-induced $[Ca^{2+}]_i$ oscillations in most δ-cells and strongly inhibited Sst secretion (**Fig. 1e-g** and **Supplementary Figs. 3 and 4**). Sst secretion involves intracellular Ca^{2+} release by a

mechanism sensitive to ryanodine and thapsigargin[8] (**Supplementary Fig. 4a**). The inhibitory effect of thapsigargin on Sst secretion correlated with an average 40% decrease in the frequency of the $[Ca^{2+}]_i$ oscillations (**Supplementary Fig. 4e**).

To distinguish between entry of extracellular Ca^{2+} and intracellular Ca^{2+} release in driving the glucose-induced $[Ca^{2+}]_i$ response, we performed parallel measurements of $[Ca^{2+}]_i$ and membrane potential in superficial δ-cells within intact islets (**Fig. 2a**). Increasing glucose resulted in membrane depolarization and initiation of action potential firing. Large $[Ca^{2+}]_i$ oscillations preceded the initiation of electrical activity and action potential firing was in fact associated with only small increases in $[Ca^{2+}]_i$. Increasing glucose also induced $[Ca^{2+}]_i$ oscillations in δ-cells voltage-clamped at -70 mV (**Fig. 2b**), an experimental paradigm leading to the abolition of spontaneous electrical activity. Although the glucose-induced $[Ca^{2+}]_i$ oscillations observed in voltage-clamped cells cannot result from action potential firing, they were strongly inhibited (fully or partially) by diazoxide (**Fig. 2b**, inset).

How can glucose induce $[Ca^{2+}]_i$ oscillations in hyperpolarised/voltage-clamped δ-cells and why are they suppressed by diazoxide? Diazoxide inhibits glucose-induced action potential firing and secretion in the β-cell[9]. We therefore hypothesized that paracrine factors (such as insulin[10] or urocortin-3[11]) released in response to electrical activity in neighbouring (unclamped) β-cells underlie the $[Ca^{2+}]_i$ oscillations in voltage-clamped δ-cells. This scenario is supported by the finding that the suppression of glucose-induced $[Ca^{2+}]_i$ oscillations by diazoxide was reversed in some δ-cells by addition of exogenous insulin (17% of δ-cells; **Fig. 2c** *i*) or urocortin-3 (9% of δ-cells; **Fig. 2c** *ii*). To restore intracellular cAMP levels in the δ-cells that may have decreased following diazoxide-induced inhibition of glucagon[12] and urocortin-3 release (both of which act by promoting cAMP production), we also tested the effects of insulin in the presence of 3 μM of forskolin. In the presence of this adenylate

cyclase activator, insulin more robustly induced $[Ca^{2+}]_i$ oscillations (27% of δ-cells; **Fig. 2c** *iii*; p=0.048 vs. no forskolin by χ^2). In the presence of forskolin, spontaneous $[Ca^{2+}]_i$ oscillations were observed in some δ-cells even before addition of insulin and the frequency of these oscillations was much higher in the simultaneous presence of insulin and forskolin than in the presence of insulin alone (0.6 min^{-1} vs 0.12 min^{-1}; p=0.01). Insulin's capacity to induce $[Ca^{2+}]_i$ oscillations in δ-cells was antagonised by dapagliflozin (an inhibitor of sodium-glucose co-transporter 2, SGLT2) in 85% of insulin-responsive cells (**Fig. 2c,** *iii-iv*). It was ascertained separately that forskolin-induced stimulation of Sst secretion was not affected by dapagliflozin in mouse and human islets (**Supplementary Fig. 5a-b**).

The effect of insulin on $[Ca^{2+}]_i$ in δ-cells correlated with stimulation of Sst release: diazoxide reduced glucose-induced Sst release by 80%, an effect reversed by application of exogenous insulin (**Fig. 2d**). Dapagliflozin abolished the stimulatory effect of exogenous insulin on Sst secretion in the presence of glucose and diazoxide (**Fig. 2d**). Although Sst release in the presence of insulin, diazoxide and glucose was not statistically lower than in islets exposed to 20 mM glucose alone (p=0.16), the mean value was 30% lower. This might reflect the component of Sst secretion resulting from δ-cell electrical activity [13] and/or urocortin-3 [11].

We next examined the role of endogenous insulin (i.e. that released from β-cells within the islets) on Sst secretion using islets from mice lacking insulin receptors in Sst-expressing cells (SIRKO mice[14]). Glucose-stimulated Sst secretion was 50% weaker in the insulin receptor-deficient islets than in control islets (**Fig. 2e**), an effect recapitulated by the insulin receptor antagonist S961 (**Supplementary Fig. 5c-d**). Dapagliflozin reduced glucose-induced Sst secretion by 70% in wild-type islets under control conditions. Sst secretion in wild-type islets in the simultaneous presence of 20 mM glucose and dapagliflozin was not statistically different (p<0.16) from that in SIRKO islets exposed to 20 mM glucose alone. Dapagliflozin

reduced somatostatin secretion in SIRKO islets but this effect did not attain statistical significance (p=0.06).

In islets exposed to 20 mM glucose, dapagliflozin inhibited Sst release with an IC_{50} of 10 nM (**Fig. 2f**). The effects of phlorizin (50 μM) on glucose-induced Sst secretion were similar to those of high concentrations of dapagliflozin (**Fig. 2g**). Part of the stimulatory effect of glucose on Sst secretion was resistant to both dapagliflozin and phlorizin, presumably reflecting the stimulation mediated by K_{ATP} channel closure. Indeed, Sst secretion in the presence of glucose and phlorizin was not higher than that elicited by 0.3 mM tolbutamide (p=0.33; **Fig. 2g**). Sst secretion elicited by this high concentration of tolbutamide (40x the K_i for the inhibitory effect on K_{ATP} channels[9]) is only 20% of that produced by 20 mM glucose, reinforcing previous arguments that depolarization as such is a weak stimulus of Sst secretion[8].

In wild-type islets exposed to 20 mM glucose, glucagon secretion was reduced by 52% compared to that observed at 1 mM glucose (**Fig. 2h**). This inhibitory effect was reversed by addition of either the Sst receptor 2 (SSTR2) antagonist CYN154806 or dapagliflozin. The combination of CYN154806 and dapagliflozin produced greater stimulation of glucagon secretion than dapagliflozin alone ($p<0.01$). Neither dapagliflozin nor CYN154806 affected glucagon or Sst secretion at 1 mM glucose (**Supplementary Fig. 6a-b**).

How does dapagliflozin inhibit Sst secretion? Electrical activity and elevation of $[Ca^{2+}]_i$ mediated glucose-induced Sst secretion. The effects of dapagliflozin on glucose-induced δ-cell electrical activity (**Supplementary Fig. 6c**) and $[Ca^{2+}]_i$ increases were inconsistent (**Supplementary Fig. 7a-b**).

There is functional and immunocytochemical evidence for the presence of SGLT2 in δ-cells[10]. To specifically activate the SGLT-expressing δ-cells, we used the non-metabolisable SGLT-specific substrate methyl-α-D-glucopyranoside (αMDG)[15]. When tested at 1 mM glucose, addition of αMDG (19 mM) stimulated Sst secretion, albeit less strongly than a corresponding increase in glucose (**Fig. 2i**). This stimulatory effect of αMDG on Sst secretion was associated with the occurrence of $[Ca^{2+}]_i$ oscillations in 37% of the δ-cells (**Fig. 3a**) without stimulation of δ-cell electrical activity (**Supplementary Fig. 6d**), suggesting they reflect intracellular Ca^{2+} release. In keeping with this idea, treatment of islets with thapsigargin largely abolished αMDG's capacity to increase $[Ca^{2+}]_i$ ($p<0.001$ compared to no thapsigargin by χ^2; **Fig. 3b**).

SGLTs mediate the uptake of glucose/αMDG by co-transport with Na^+ down its electrochemical gradient. We explored the significance of the transmembrane Na^+ gradient for the effects of αMDG on δ-cell $[Ca^{2+}]_i$ by lowering the extracellular Na^+ concentration ($[Na^+]_o$) from the normal 140 mM to 10 mM. This reduced both the αMDG-induced $[Ca^{2+}]_i$ oscillations (**Fig. 3a**) and αMDG- and glucose-induced Sst secretion (**Fig. 2i**). The inhibitory effect of Na^+ removal on glucose-induced Sst secretion was comparable to that produced by dapagliflozin in control islets (*cf.* **Fig. 2e**). Addition of αMDG increased $[Na^+]_i$ in 39% of the δ-cells (**Fig. 3c-d** and **Supplementary Fig. 6e**), in agreement with the fraction of δ-cells in which $[Ca^{2+}]_i$ oscillations were induced by αMDG (37%; see above). When αMDG was applied in the presence of 100 nM dapagliflozin, the increase in $[Na^+]_i$ was abolished (**Fig. 3c-d**). Dapagliflozin (1 nM-1 μM) also prevented the insulin-dependent potentiation of the αMDG-induced increase in $[Na^+]_i$ (**Fig 3e-f** and **Supplementary Fig. 8**).

We hypothesised that the increase in $[Na^+]_i$ triggers CICR by producing a small increase in $[Ca^{2+}]_i$. This idea is supported by our finding that application of the Na^+ ionophore monensin initiated $[Ca^{2+}]_i$ oscillations (**Fig. 3g**). The oscillations evoked by monensin persisted for >30 min and were resistant to a cocktail of diazoxide and the Ca^{2+} channel blockers isradipine and SNX482 (**Fig. 3g** and **Supplementary Fig. 9a**) and independent of electrical activity (**Fig. 3b** and **Supplementary Fig. 9b**).

Lowering $[K^+]_o$ inhibits the plasmalemmal Na^+/K^+ pump[16] and it is therefore expected to increase $[Na^+]_i$. Insulin's hypokalaemic (i.e. reduction of plasma K^+) action is well established and has been attributed to stimulation of K^+ uptake in skeletal muscle[17]. In mice, insulin (0.75 U/kg) lowered plasma $[K^+]$ from 5.0±0.7 to 3.0±0.3 mM (**Fig. 3h**), comparable to that reported in patients with type 1 diabetes[6]. Notably, plasma $[K^+]$ fell to values <4 mM in all mice and <2.7 mM in 3 of 5 mice. Lowering $[K^+]_o$ to 2.7 mM increased $[Na^+]_i$ in δ-cells (**Fig. 3i-j**). This increase in $[Na^+]_o$ was associated with the induction of $[Ca^{2+}]_i$ oscillations in 72% of δ-cells in islets exposed to 1 mM glucose (**Fig. 3k**).

At 1 mM glucose, δ-cells are hyperpolarized and do not generate action potentials. Reducing $[K^+]_o$ to 1.7 mM promptly produced an additional 7±1 mV hyperpolarization (n=3: measured 5 min after switching to the lower $[K^+]_o$). The resting membrane potential of the δ-cell is determined by K_{ATP} channel activity[18] and depends on $[K^+]_o$ (**Supplementary Fig. 9d**). We determined the effect of reduced $[K^+]_o$ on glucagon and Sst secretion. Despite its hyperpolarising effect, lowering $[K^+]_o$ from 4.7 mM to 3.7 mM stimulated Sst secretion in islets exposed to 6 mM glucose; no further stimulation was observed at 2.7 or 1.7 mM (**Fig. 4a**). A stimulatory effect was also observed at 1 mM glucose but in this case a reduction to ≤2.7 mM was required (**Fig. 4a**). The stimulation of Sst secretion was associated with progressive inhibition of glucagon secretion at both 1 and 6 mM (**Fig. 4b**). We found that

CYN154806 reversed the inhibitory effect of 1.7 mM $[K^+]_o$ at both 1 mM or 6 mM glucose (**Fig. 4c**). Thus, the insulin-induced reductions of plasma K^+ are likely to be associated with stimulation of Sst secretion under both normoglycaemic (6 mM) and severely 'hypoglycaemic' (1 mM) conditions *in vitro*.

Type-2 diabetes (T2DM) is associated with impaired glucose-induced insulin secretion and dysregulation of glucagon secretion[12,19] but whether Sst secretion is also affected is not known. We studied Sst and glucagon in hyperglycaemic Fh1βKO mice, a model of progressive β-cell failure associated with marked suppression of glucagon secretion[20]. In control islets, Sst secretion at 1 mM glucose was low and stimulated >10-fold at 20 mM glucose. In islets from hyperglycaemic Fh1βKO mice, Sst secretion at 1 mM glucose was increased 6-fold compared to control islets (echoing previous observations in diabetic dogs and rats[21,22]) and 20 mM glucose was without a statistically significant stimulatory effect (**Fig. 4d**). This correlated with a >75% reduction of glucagon secretion at 1 mM glucose ($p<0.05$; **Fig. 4e**). Consistent with an increased Sst tone at 1 mM glucose, addition of CYN154806 increased glucagon secretion by 143±11% in Fh1βKO mice but only 13±14% in controls ($p=0.022$).

We extended these data to human islets. In islets from non-diabetic donors (ND), Sst secretion was low at 1 mM glucose and stimulated >3-fold by 20 mM glucose (**Fig. 4f**). In contrast, glucose was without stimulatory effect in islets from donors with T2DM. Interestingly, there was a trend ($p<0.06$) towards elevated Sst release at 1 mM glucose, similar to that observed in Fh1βKO islets. There was no difference in Sst content in islets from diabetic and non-diabetic donors (**Supplementary Fig. 10a**). In T2DM islets, glucagon secretion at 1 mM glucose was on average 65% lower than observed in ND preparations (**Fig. 4g**), despite glucagon content was 200% higher in T2DM islets (**Supplementary Fig. 10b**).

We tested whether Sst receptor antagonists can restore glucagon secretion at low glucose in a small number of human T2DM islet preparations. We found that the SSTR2 antagonist CYN154806 increased glucagon secretion at 1 mM glucose in two preparations with low glucagon secretion. In a third preparation with higher glucagon secretion, CYN154806 had no effect (**Fig. 4h**). Extrapolating from our findings in islets from mice we propose that the stimulatory effect of the SSTR2 antagonist in T2DM islets reflects hypersecretion of Sst at low glucose concentrations. This conclusion is reinforced by electrophysiological measurements in intact human pancreatic islets demonstrating transient and CYN154806-sensitive membrane hyperpolarizations in T2DM but not in ND α-cells (**Supplementary Fig. 10c-e**).

The schematic in **Fig. 4i** combines these findings into a model for glucose-induced Sst secretion that incorporates K_{ATP} channels, the Na^+/K^+ pump, voltage-gated Ca^{2+} channels and intracellular Ca^{2+}-induced Ca^{2+} release (CICR). Glucose- and insulin-dependent Na^+ uptake is sufficient to trigger CICR and Sst secretion in δ-cells even in the absence of electrical activity. The effects of dapagliflozin in δ-cells were observed at 1-10 nM, concentrations adequate to suppress SGLT2 activity but too low to inhibit SGLT1[23]. However, the expression of *Slc5a2* (which encodes SGLT2) is low in mouse δ-cells and that of *Slc5a1* (encoding SGLT1) is higher (although still lower than transcripts encoding GLUT1-3; see **Supplementary Table 1** and [24]). The low expression of SGLT1/2 would be in agreement with the small size of the current (~1 pA) in δ-cells inhibited by high (μM) concentrations of dapagliflozin[14]. In kidney cells, insulin selectively activates SGLT2 (via an effect involving protein phosphorylation) with little effect on SGLT1[25] but it remains possible that SGLT1 is insulin-sensitive in δ-cells. Dapagliflozin has been reported to stimulate glucagon secretion both *in vitro*[26] and *in vivo*[27] (but see [24]). Our data suggest that the stimulation of glucagon

secretion is secondary to the suppression of Sst secretion, resulting in removal of paracrine suppression of α-cells. Given the low expression of *Slc5a2* in δ-cells, the possibility that the dapagliflozin-induced suppression of Sst secretion reflects an off-target SGLT2-independent effect remains possible, similar to what was recently reported for the related compound canagliflozin[28]. Ultimately, to conclusively demonstrate that SGLT1 or 2 are functional in δ-cells, studies would need to be conducted using δ-cell-specific ablation of *Slc5a1* and/or *Slc5a2*.

Despite the uncertainty about the molecular identity of the transporter mediating Na^+ and glucose uptake into δ-cells, it is clear that the mechanisms involved culminate in elevation of $[Na^+]_i$, which accounts for the Na^+-dependent ability of the non-metabolisable glucose analogue αMDG to evoke $[Ca^{2+}]_i$ oscillations and Sst release by promoting CICR, in agreement with previously reported stimulatory effects of 3-O-methyl-D-glucose on Sst secretion[29]. It is notable that inhibition of the plasmalemmal Na^+/Ca^{2+} (NCX) by reduction of $[Na^+]_o$ leads to a reduction of Ca^{2+} in δ-cells (i.e. the opposite to what we observe and unlike the increase seen in β-cells[30]). We therefore propose that the αMDG/glucose-induced increase $[Na^+]_i$ is mediated by activation of intracellular Na^+/Ca^{2+} exchange (like NCLX[31]) rather than inhibition of NCX. The resulting small/initial increase in δ-cell $[Ca^{2+}]_i$ thus produced leads to further mobilization of Ca^{2+} from intracellular stores (including the sER) by activation of CICR, explaining why the effect of αMDG on $[Ca^{2+}]_i$ was almost abolished after pretreatment with thapsigargin. The model explains why glucose is a stronger stimulus of Sst secretion than αMDG. Unlike αMDG, which exclusively acts by increasing $[Na^+]_i$, glucose also causes K_{ATP} channel closure. Thus, elevation of $[Na^+]_i$ represents one important intracellular messenger – but not the only one - linking elevated plasma glucose to stimulation of Sst secretion.

Our findings suggest that exogenous insulin may not only lead to hypoglycaemia by stimulating glucose uptake but also interfere with the defences against hypoglycaemia by producing hypokalaemia by stimulation of Sst secretion (via inhibition of the Na-K pump and elevation of $[Na^+]_i$) and suppression of glucagon secretion. It is intriguing that the effects of T2DM on Sst secretion resemble those produced by lowering of $[K^+]_o$: namely increased basal Sst secretion and impaired stimulation by high glucose. Our data raise the interesting possibility that SGLT2 inhibitors – regardless of their exact mode of action - may correct the Sst secretion defects associated with diabetes, thereby restoring counter-regulatory glucagon secretion and reducing the risk of fatal hypoglycaemia[4]. 2860 words

Materials and Methods

Ethics

All animal experiments were conducted in accordance with the UK Animals Scientific Procedures Act (1986) and ethical guidelines of the universities of Oxford, Lund and Gothenburg and were approved by the respective local Ethical Committees. Human pancreatic islets were isolated, with ethical approval and clinical consent, at the Diabetes Research and Wellness Foundation Human islet Isolation Facility (Oxford) and the Alberta Diabetes Institute IsletCore (Edmonton, Canada). Details on the donors are provided in **Supplementary Table 2.**

Mouse models

In this study, mice expressing GCaMP3 and/or RFP under the Sst promoter (Sst-Cre-GCaMP3 and Sst-Cre-RFP mice, respectively) were used. These mice were generated as previously described[32]. The generation of mice lacking insulin receptors in Sst-secreting δ-cells (SIRKO mice) have been reported elsewhere[14]. Fh1βKO mice were generated as previously described[33].

Intraperitoneal glucose tolerance test

Blood glucose levels were measured using the Accu-Check Aviva from a drop of blood obtained by a tail vein nick. For these experiments, 12-20 weeks old mice were used. Mice were fed ad libitum and fed blood glucose levels were measured prior to fasting. For the GCaMP3 experiments, mice were fasted overnight (16 h). A bolus of glucose (2g per kg of body weight, Sigma) was injected intraperitoneally (ip) with a 25-gauge needle at time 0.

Blood glucose levels were measured at intervals of 0, 15, 30, 60, 90, 120 and 150 min after ip glucose administration.

Plasma K^+ measurements

Plasma K^+ concentrations were measured with a micro-ion potassium selective electrode (LIS-146KCM), micro reference electrode (LIS DJM146) and a 6230N Ion meter (Lazar Research Laboratories, Inc., USA). K^+ standard solutions were prepared by diluting 0.1 M standard KCl to concentrations between 0.1 and 100 mM KCl. Both the K^+ and reference electrodes were placed in the standard solutions and the voltage determined. The K^+ and references electrodes were washed and wiped between each measurement. The insulin tolerance tests were performed in C57Bl6j mice. Blood samples were obtained at t=0 and t=45 min after injection of insulin. The blood cells were removed and plasma frozen pending later analysis. Plasma samples were diluted 20x to a final volume of 100 µl and injected into clean well plates and measurements were conducted as above.

Pancreatic islets isolation

Mice (16-24 weeks old) were killed by cervical dislocation, the pancreases quickly removed and islets isolated either by collagenase (Sigma) or liberase (Roche) digestion.

Immunocytochemistry

Immunocytochemistry was performed as previously described[14]. The primary antibodies used in this study were: rabbit anti-somatostatin (Sigma, 1:250), Guinea pig anti-insulin (Sigma, 1:3000), mouse anti-glucagon (Sigma, 1:4000), chicken anti-GFP (Invitrogen, 1:500). The secondary antibodies were all from Invitrogen (1:500).

Flow cytometry of islet cells (FACS)

Pancreatic islets from Sst-Cre-GCaMP3 mice were dissociated into single cells by trypsin digestion and mechanical dissociation as described previously[14] and filtered through a 30 μm filter to remove remaining clumps of cells.

Single cells were passed through a MoFlo Legacy (Beckman Coulter). GCaMP3- or RFP-positive cells were purified by combining several narrow gates. Forward and side scatter were used to isolate small cells and to exclude cell debris. Cells were then gated on pulse width to exclude doublets or triplets. GCaMP3-positive cells were excited with a 488 nm laser and the fluorescent signal was detected through a 530/40 nm bandpass filter (*i.e.* in the range 510-550 nm). RFP was excited with the 488 nm laser and the fluorescent signal was detected through a 580/30 nm bandpass filter (*i.e*. in the range 565-595nm). GCaMP3- or RFP-negative cells were collected in parallel.

RNA extraction, cDNA synthesis and quantitative PCR

The levels of gene expression in the positive and in the negative FAC-sorted fractions were determined using real-time quantitative PCR (qPCR). Total RNA was extracted using RNeasy Micro Kit (Qiagen) and cDNA was synthesised using High Capacity RNA-to-cDNA™ Kit (Applied Biosystem).

qPCR was performed using SYBR Green kit (QuantiFast SYBR Green PCR Kit, Qiagen) and ABI 7900HT Sequence Detection System (Applied Biosystems). Primers used were QuantiTect Primer Assays: QT00114289 (Ins2), QT00124033 (Gcg), QT00239295 (Sst), QT00095242 (Actb). Each sample was run in duplicate or triplicate. Differences in expression of target genes in the GCaMP3 positive/negative were calculated using the $2^{\Delta\text{-}\Delta CT}$ method[34].

Secretion measurements

Freshly isolated islets were used in static secretion experiments. These experiments were performed as described previously[10].

Two different extracellular solutions (ES) were used for the various experiments: ES1 contained (mM) 120 NaCl, 4.7 KCl, 2.5 $CaCl_2$, 25 $NaHCO_3$, 1.2 KH_2PO_4, 1.2 $MgSO_4$, 10 HEPES and 0.1% BSA (pH=7.4 with NaOH and bubbled with 95:5% O_2:CO_2). For some experiments (to allow correlation with electrophysiology and $[Ca^{2+}]_i$ imaging when 'bubbling' with O_2:CO_2 is not feasible), a modified extracellular medium (ES2) that equilibrates with atmospheric CO_2 levels was used. It consisted of (mM) 140 NaCl, 4.7 KCl, 2 $NaHCO_3$, 0.5 NaH_2PO_4, 0.5 $MgSO_4$, 5 HEPES, 1.5-2.6 $CaCl_2$ (EC1) and 0.1% BSA (pH=7.4 with NaOH). Secretion data obtained with the two different media were essentially identical.

All experiments were carried out in a shaking water bath at 37ºC. Groups of 15-20 islets from at least three mice were pooled together and used in each experiment. When extracellular $[Na^+]$ was lowered to 10 mM, the extracellular solution was compensated with choline chloride to maintain iso-osmolarity.

All chemicals used in this study were from Sigma (UK) with the following exception: isradipine and SNX-482 were from Alomone (Jerusalem, Israel); ryanodine, thapsigargin and CYN154806 were from Tocris (Abingdon, UK) and dapagliflozin was from Cayman Bioscience (Cambridge, UK). S961 was from Sigma-Aldrich.

Samples were assayed by radioimmunoassay (RIA). The kits for glucagon and somatostatin were from Millipore (USA) and Eurodiagnostica (Malmö, Sweden), respectively. The somatostatin RIA from Eurodiagnostica was discontinued and two series of experiments (**Fig.**

2f-g) were instead analysed using a RIA from Diasource (P/N RB306RUO; Louvain-la-Neuve, Belgium). The assay provided by the latter supplier indicated higher basal (1 mM glucose) Sst release and this may be the reason that the fold stimulation produced by glucose is lower in these experiments.

For unknown reasons, glucagon secretion rates vary between different laboratories and/or assays. Human glucagon secretion data reported here include only experiments performed in Oxford. This is the explanation why glucagon secretion at 1 mM glucose now reported is lower than that presented in a previous study (which included experiments conducted in two different laboratories)[12]. Because the experiments were performed in two different laboratories and over many years, secretion data have been expressed relative glucagon or somatostatin secretion at 1 mM glucose.

Pancreas perfusion

In situ measurements of glucagon secretion were performed using the perfused mouse pancreas. Briefly, the aorta was ligated above the coeliac artery and below the superior mesenteric artery and then cannulated. The pancreas was perfused with KRB containing glucose and CYN154806 at a speed of 0.24 ml/min using an Ismatec Reglo Digital MS2/12 peristaltic pump. The perfusate was maintained at 37°C using a Warner Instruments temperature control unit TC-32 4B in conjunction with a tube heater (Warner Instruments P/N 64-0102) and a Harvard Apparatus heated rodent operating table. The effluent was collected in intervals of 1 min. Samples were subsequently stored at -80°C. Glucagon content in perfusate were measured using U-plex glucagon ELISA (Meso Scale Discovery), according to the manufacturer's protocol.

Intracellular [Ca^{2+}] measurements

$[Ca^{2+}]_i$ measurements were performed as described previously[35]. Islets were imaged in a heated chamber at 37ºC placed on an inverted LSM510 confocal microscope (Zeiss; Oberkochen, Germany) using a 40X oil objective (NA1.4). The pinhole diameter was kept constant, and frames of 256x256 pixels were taken every 1-3 s.

Parallel measurement of membrane potential and $[Ca^{2+}]_i$

The electrophysiological measurements were performed in intact islets essentially using the perforated-patch whole-cell technique in the voltage- or current-clamp modes in δ-cells.

Parallel measurements of $[Ca^{2+}]_i$ and membrane potential were performed using an Axioskop 2FS microscope (Zeiss, Oberkochen, Germany) equipped with a 40x/0.8 objective, Lambda DG-4 exciter (Sutter Instruments, USA) and Orca-R2 cooled CCD camera (Hamamatsu, Japan). Images were acquired using an open-source Micromanager software (developed at Ron Vale's lab, UCSF, San Francisco, USA) and processed using ImageJ. Data analysis was performed in Igor Pro (Wavemetrics).

Intracellular Na^+ and pH measurements

Time-lapse imaging of $[Na^+]_i$ in dispersed mouse islets was performed on a Zeiss Axiozoom.V16 microscope. Cells were pre-loaded with 6 μM of Sodium Green (Molecular Probes) for 30 min at room temperature and imaged at several locations simultaneously. Sodium Green was excited at 490 nm and emission was collected at 515 nm, using a CCD camera. Time-lapse images were collected every 60 s and the bath solution was superfused at 60 μl/min, at 34°C. δ-cells were identified by the RFP fluorescence. Images were acquired using ZenBlue software (Carl Zeiss). Imaging of pH_i in GCamP3-expressing δ-cells was performed on an inverted Zeiss AxioVert 200 microscope equipped with Zeiss 510-META

laser confocal scanning system, using 40x/1.3 objective. Cells were loaded with 6 μM of the pH-sensitive dye SNARF-5F for 50 min at room temperature. SNARF-5F was excited at 543 nm and emission was collected at 650 nm and 600 nm.

Statistical analysis

Calcium imaging videos were analysed using a combination of Fiji and IgorPro. Briefly, an in-house macro was used to auto-detect GCaMP3-expressing regions of interest representing individual δ-cells. The mean fluorescent intensities of these regions of interest were exported to IgorPro for individual wave plotting of each δ-cell. The mean fluorescent intensities were expressed as F/F_0 and transformed using a Mexican hat filter and Fourier scaling for baseline correction. AUC and spike frequency detection methods in IgorPro were then employed to quantify these parameters for each δ-cell. The AUC and spike frequency data were compared back to the raw traces visualised in Fiji to confirm accuracy and faithful representation of the raw data.

GraphPad Prism 6.0 software was used for statistical analysis. Differences between two groups were assessed by two-tailed unpaired Student's *t*-test while for differences between more groups one-way ANOVA or two-way ANOVA followed by a post hoc test were used. Data are presented as mean values ± S.E.M.

Data availability

The data that support the findings of this study are available from the corresponding authors upon request.

Acknowledgements

EV was supported by the OXION Wellcome Training Programme and LB by a Sir Henry Wellcome Postdoctoral Fellowship. QZ, AH, RR were supported by Diabetes UK. Work in Oxford was supported by the Wellcome, Diabetes UK and the European Foundation for the Study of Diabetes. Work in Sweden was supported by the Diabetes Research and Wellness Foundation, the Swedish Research Council and The Knut and Alice Wallenbergs Stiftelse.

Author contribution

EV, LJBB and PR designed experiments. EV, AA, AB, MC, GD, TGH, CG, AH, FR, RR, NJGR, AS, IS, AIT, QZ, JNW and IWA, research and analysed data. PR and LJBB wrote the paper. All co-authors read and approved of the final version of the manuscript.

Competing interests

The authors have no competing interests.

References

1. Dolensek, J., Rupnik, M.S. & Stozer, A. Structural similarities and differences between the human and the mouse pancreas. *Islets* **7**, e1024405 (2015).
2. Hauge-Evans, A.C.*, et al.* Somatostatin secreted by islet delta-cells fulfills multiple roles as a paracrine regulator of islet function. *Diabetes* **58**, 403-411 (2009).
3. Yue, J.T.*, et al.* Somatostatin receptor type 2 antagonism improves glucagon and corticosterone counterregulatory responses to hypoglycemia in streptozotocin-induced diabetic rats. *Diabetes* **61**, 197-207 (2012).
4. Cryer, P.E. Mechanisms of hypoglycemia-associated autonomic failure and its component syndromes in diabetes. *Diabetes* **54**, 3592-3601 (2005).
5. Rorsman, P. & Huising, M.O. The somatostatin-secreting pancreatic delta-cell in health and disease. *Nat Rev Endocrinol* **14**, 404-414 (2018).
6. Caduff, A.*, et al.* Dynamics of blood electrolytes in repeated hyper- and/or hypoglycaemic events in patients with type 1 diabetes. *Diabetologia* **54**, 2678-2689 (2011).
7. Adriaenssens, A.E.*, et al.* Transcriptomic profiling of pancreatic alpha, beta and delta cell populations identifies delta cells as a principal target for ghrelin in mouse islets. *Diabetologia* **59**, 2156-2165 (2016).
8. Zhang, Q.*, et al.* R-type Ca(2+)-channel-evoked CICR regulates glucose-induced somatostatin secretion. *Nat Cell Biol* **9**, 453-460 (2007).
9. Trube, G., Rorsman, P. & Ohno-Shosaku, T. Opposite effects of tolbutamide and diazoxide on the ATP-dependent K+ channel in mouse pancreatic beta-cells. *Pflugers Arch* **407**, 493-499 (1986).
10. Vergari, E.*, et al.* Insulin inhibits glucagon release by SGLT2-induced stimulation of somatostatin secretion. *Nature Communications* **10**, 139 (2019).
11. van der Meulen, T.*, et al.* Urocortin3 mediates somatostatin-dependent negative feedback control of insulin secretion. *Nat Med* **21**, 769-776 (2015).
12. Zhang, Q.*, et al.* Role of KATP channels in glucose-regulated glucagon secretion and impaired counterregulation in type 2 diabetes. *Cell Metab* **18**, 871-882 (2013).
13. Briant, L.J.B.*, et al.* delta-cells and beta-cells are electrically coupled and regulate alpha-cell activity via somatostatin. *J Physiol* **596**, 197-215 (2018).
14. Vergari, E.*, et al.* Insulin inhibits glucagon release by SGLT2-induced stimulation of somatostatin secretion. *Nat Commun* **10**, 139 (2019).
15. Wright, E.M., Loo, D.D. & Hirayama, B.A. Biology of human sodium glucose transporters. *Physiol Rev* **91**, 733-794 (2011).
16. Henquin, J.C. & Meissner, H.P. The electrogenic sodium-potassium pump of mouse pancreatic B-cells. *J Physiol* **332**, 529-552 (1982).
17. Unwin, R.J., Luft, F.C. & Shirley, D.G. Pathophysiology and management of hypokalemia: a clinical perspective. *Nature reviews. Nephrology* **7**, 75-84 (2011).
18. Denwood, G.*, et al.* Glucose stimulates somatostatin secretion in pancreatic delta-cells by cAMP-dependent intracellular Ca(2+) release. *J Gen Physiol* (2019).
19. Rosengren, A.H.*, et al.* Reduced insulin exocytosis in human pancreatic beta-cells with gene variants linked to type 2 diabetes. *Diabetes* **61**, 1726-1733 (2012).

20. Knudsen, J.G.*, et al.* Dysregulation of Glucagon Secretion by Hyperglycemia-Induced Sodium-Dependent Reduction of ATP Production. *Cell Metab* **29**, 430-442 e434 (2019).
21. Abdel-Halim, S.M., Guenifi, A., Efendic, S. & Ostenson, C.G. Both somatostatin and insulin responses to glucose are impaired in the perfused pancreas of the spontaneously noninsulin-dependent diabetic GK (Goto-Kakizaki) rats. *Acta Physiol Scand* **148**, 219-226 (1993).
22. Hermansen, K. Characterisation of the abnormal pancreatic D and A cell function in streptozotocin diabetic dogs: studies with D-glyceraldehyde, dihydroxyacetone, D-mannoheptulose, D-glucose, and L-arginine. *Diabetologia* **21**, 489-494 (1981).
23. Ghezzi, C., Loo, D.D.F. & Wright, E.M. Physiology of renal glucose handling via SGLT1, SGLT2 and GLUT2. *Diabetologia* **61**, 2087-2097 (2018).
24. Kuhre, R.E.*, et al.* No direct effect of SGLT2 activity on glucagon secretion. *Diabetologia* **62**, 1011-1023 (2019).
25. Ghezzi, C. & Wright, E.M. Regulation of the human Na+-dependent glucose cotransporter hSGLT2. *Am J Physiol Cell Physiol* **303**, C348-354 (2012).
26. Bonner, C.*, et al.* Inhibition of the glucose transporter SGLT2 with dapagliflozin in pancreatic alpha cells triggers glucagon secretion. *Nat Med* **21**, 512-517 (2015).
27. Ferrannini, E.*, et al.* Metabolic response to sodium-glucose cotransporter 2 inhibition in type 2 diabetic patients. *J Clin Invest* **124**, 499-508 (2014).
28. Hawley, S.A.*, et al.* The Na+/Glucose Cotransporter Inhibitor Canagliflozin Activates AMPK by Inhibiting Mitochondrial Function and Increasing Cellular AMP Levels. *Diabetes* **65**, 2784-2794 (2016).
29. Hermansen, K., Lindskog, S. & Ahren, B. Stimulation of somatostatin secretion by 3-O-methylglucose in the perfused dog pancreas. *Int J Pancreatol* **20**, 103-107 (1996).
30. Rorsman, P., Ammala, C., Berggren, P.O., Bokvist, K. & Larsson, O. Cytoplasmic Calcium Transients Due to Single Action-Potentials and Voltage-Clamp Depolarizations in Mouse Pancreatic B-Cells. *Embo Journal* **11**, 2877-2884 (1992).
31. Palty, R.*, et al.* NCLX is an essential component of mitochondrial Na+/Ca2+ exchange. *P Natl Acad Sci USA* **107**, 436-441 (2010).
32. Chera, S.*, et al.* Diabetes recovery by age-dependent conversion of pancreatic delta-cells into insulin producers. *Nature* **514**, 503-507 (2014).
33. Adam, J.*, et al.* Fumarate Hydratase Deletion in Pancreatic beta Cells Leads to Progressive Diabetes. *Cell Rep* **20**, 3135-3148 (2017).
34. Schmittgen, T.D. & Livak, K.J. Analyzing real-time PCR data by the comparative C(T) method. *Nat Protoc* **3**, 1101-1108 (2008).
35. Briant, L.J.B.*, et al.* CPT1a-Dependent Long-Chain Fatty Acid Oxidation Contributes to Maintaining Glucagon Secretion from Pancreatic Islets. *Cell Rep* **23**, 3300-3311 (2018).

Figure Legends

Figure 1. Regulation of somatostatin secretion by Ca^{2+}. *a*, Glucose-induced $[Ca^{2+}]_i$ oscillations in 3 representative δ-cells (n=79 cells from 7 mice). *b-c*, Somatostatin secretion (*b*) and frequency of $[Ca^{2+}]_i$ oscillations (*c*) measured at 1, 4 and 20 mM glucose (n=61-79 cells/7 islets/7 mice). 1-way ANOVA with Tukey adjustment. *d-g*, Frequency of $[Ca^{2+}]_i$ oscillations in the absence or presence of tolbutamide (*d*; n=48 cells/3 mice; 2-sided t-test), diazoxide (*e*; n=13 cells/3 mice, 1-way RM ANOVA with Tukey adjustment), isradipine (*f*; n=22 cells/3 mice, 1-way RM ANOVA with Tukey adjustment) and SNX482 (*g*; n=22 cells/3 mice, 1-way RM ANOVA with Tukey adjustment). *p<0.05, **p<0.005, ***p<0.001 vs 1 mM glucose; †††p<0.001 vs 20 mM glucose. All data are represented as mean ± SEM.

Figure 2. Insulin-induced intracellular Ca^{2+} mobilization. *a*, Parallel measurements of membrane potential (V_m) and $[Ca^{2+}]_i$ in a δ-cell recorded at 1 and 10 mM glucose (representative of 4 experiments). Dotted vertical lines have been inserted to highlight the lack of correlation between V_m and $[Ca^{2+}]_i$. *b*, As in (*a*) but in a δ-cell voltage-clamped at -70 mV. Diazoxide was included as indicated (red). It was ascertained by application of a 500-ms voltage-clamp pulse from -70 to 0 mV (left) that the $[Ca^{2+}]_i$ measurements reflect the voltage-clamped cells (representative of 3 experiments). Scatter graph (inset) summarizes effects of 1 mM glucose (open circle), 20 mM glucose (open square) and 20 mM glucose with 100 μM diazoxide (open triangle) on $[Ca^{2+}]_i$ (AUC). 1-way RM ANOVA with Tukey adjustment, n=4 cells/3 mice. *c*, (Top): Bar graphs summarising the frequencies of $[Ca^{2+}]_i$ oscillations in the absence or presence of (*i)* insulin (Ins; 100 nM), (*ii)* urocortin-3 (UCN3; 100 nM) and (*iii)* insulin (100 nM), forskolin (3 μM) and dapagliflozin (100 nM: Ins+Fsk) all in the continued presence of 20 mM glucose and 100 μM diazoxide. 1-way RM ANOVA with Tukey adjustment; *p<0.05, **p<0.01, ***p<0.001. The pie charts indicate the % of cells

responding to each of these conditions (total number of cells are indicated; from 2-3 mice). *iv*, Insulin-induced $[Ca^{2+}]_i$ oscillations in the presence of forskolin and their suppression by dapagliflozin. *d*, Somatostatin secretion measured in the presence of glucose, diazoxide, insulin and dapagliflozin as indicated (n=5 experiments/3 mice). 1-way ANOVA with Tukey adjustment; ***p<0.001 *vs.* 1 mM glucose; ††p<0.01, †††p<0.05, *vs.* 1 mM glucose. *e*, Somatostatin secretion (after normalization to somatostatin content) measured in control and SIRKO mice at 1 and 20 mM glucose in the absence and presence of dapagliflozin as indicated (n=5 experiments/3 mice). 1-way ANOVA with Tukey adjustment; *p<0.05, **p<0.01, †p<0.05. *f*, Somatostatin secretion at 1 and 20 mM glucose (as indicated) and increasing concentrations of dapagliflozin (n=10 experiments/7 mice). The curve was derived by fitting the function y = base – (base-min) /(1 + (x_{50}/x)^rate) to the mean values (base =2.5, min=1.4, x_{50} = 10 nM and rate=-1). *g*, Somatostatin secretion at 1 and 20 mM glucose and phlorizin (50 μM) as indicated (n=7-10 experiments/7 mice). 1-way ANOVA with Tukey adjustment; *p<0.05, **p<0.01 *vs.* 1 mM glucose; †p<0.01 *vs.* 20 mM glucose. *h*, glucagon secretion in the presence of glucose, dapagliflozin and CYN154806 as indicated (n=6-9 experiments/3 mice). 1-way ANOVA with Tukey adjustment; ***p <0.0005 *vs.* 1 mM glucose; ††p<0.01 *vs.* 20 mM glucose; ‡‡p<0.01 *vs.* 20 mM glucose with 12.5 μM dapagliflozin. *i*, Somatostatin secretion measured in the presence of glucose, αMDG and $[Na^+]_o$ as indicated (n=8 experiments/3 mice). 1-way ANOVA with Tukey adjustment; ***p <0.0005 *vs.* 1 mM glucose; †p<0.05, *vs.* 1 mM glucose with 19 mM αMDG and 140 mM $[Na^+]_o$; ‡‡‡p<0.01 *vs.* 20 mM glucose with 140 mM $[Na^+]_o$. All data are represented as mean ± SEM.

Figure 3. Elevation of cytoplasmic Na^+ stimulates somatostatin release. *a*, Effects of αMDG applied at 1 mM glucose on δ-cell $[Ca^{2+}]_i$ and impact of lowering $[Na^+]_o$ as indicated (72 of

182 cells in 8 islets from 6 mice). *b*, As in (*a*) but αMDG applied in islets pretreated for 90 min with thapsigargin (oscillations observed in 4 of 34 cells in 3 islets from 3 mice). *c*, Effects of αMDG on $[Na^+]_i$ measured in dispersed δ-cells applied at 1 mM glucose in the absence and presence of 100 nM dapagliflozin (Dapa) as indicated. Trace representative of αMDG-responding δ-cells (53 of 136 cells). The fluorescence (F) has been normalised to the initial signal (F_0) in the subset of cells responding to αMDG. *d*, Bar graph summarising effects of αMDG and dapagliflozin on $[Na^+]_i$. Mean values ± S.E.M. in 53 of 136 cells from 4 mice (only the subset of cells responding to αMDG were included in these analyses). *p<0.05. *e-f*, As in *c-d* but in the presence of 100 nM insulin and 1 nM dapagliflozin (Dapa). The dotted line shows data for insulin-unresponsive cells. Data in *f* are mean values ± S.E.M. in of 36 insulin-responsive δ-cells from 2 mice. *g,* $[Ca^{2+}]_i$ measured in a δ-cell induced by monensin (50 μM) applied at 1 mM glucose and lack of effects of a cocktail of diazoxide (0.1 mM), SNX482 (100 nM) and isradipine (2.5 μM) (shaded area). *h*, Plasma K^+ measured in mice before and 45 min after intraperitoneal injection of 0.75 U/kg body weight insulin. Paired t-test; *p<0.05 (n=5 mice). Plasma glucose fell from 7.4±0.6 to 3.7±0.7 mM (n=5 mice) ~~(data not shown)~~. *i-j*, As in *c-d* but measuring the effect of lowering $[K^+]_o$ from 4.7 to 2.7 mM. Bar graph in (*j*) shows mean value ± S.E.M of 231 cells from 4 mice. All cells were included in this analysis. Paired t-test; ***p<0.001. *k*, $[Ca^{2+}]_i$ oscillations induced at 1 mM glucose by lowering $[K^+]_o$ to 2.7 mM (representative of 16 cells in 3 islets from 2 mice). All data are represented as mean ± SEM.

Figure 4. Effects of hypokalaemia and type-2 diabetes on glucagon and somatostatin secretion. *a-b*, Somatostatin (*a*) and glucagon secretion (*b*) at 1 mM (black) and 6 mM (red) glucose at the indicated $[K^+]_o$. 1-way ANOVA with Tukey adjustment; †p<0.05; ††p<0.01; †††p<0.001 *vs.* 1 mM glucose at 4.7 mM $[K^+]_o$. Effects of increasing glucose from 1 to 6 mM

is statistically significant at 4.7, 3.7 and 2.7 mM $[K^+]_o$; *p<0.05; **p<0.01 and ***p<0.001. Mean values ± S.E.M of n=12 experiments/6 mice. *c*, Glucagon secretion at 1 or 6 mM glucose and at 4.7 or 1.7 mM $[K^+]_o$ in the absence or presence of CYN154806 (CYN) as indicated. 1-way ANOVA with Tukey adjustment; ***p<0.001 *vs.* 1 mM glucose at 4.7 mM $[K^+]_o$; †††p<0.001 *vs.* 1 mM glucose at 1.7 mM $[K^+]_o$; ‡‡p<0.005 *vs.* 1 mM glucose at 1.7 mM $[K^+]_o$ in the presence of CYN154806 (n=9 experiments/4 mice). *d*, Somatostatin secretion in islets from control (CTL) and hyperglycaemic Fh1βKO (KO) mice at 1 and 20 mM glucose (n=4-5 using islets from 4 mice). 1-way ANOVA with Tukey adjustment; **p<0.01 vs 1 mM glucose; †p<0.05 *vs.* 1 mM glucose in CTL islets. *e*, Glucagon secretion from the perfused mouse pancreas of CTL (n=5) and hyperglycaemic Fh1βKO (KO, n=4) mice at 1 mM glucose in the absence and presence of CYN154806 as indicated. 1-way ANOVA with Tukey adjustment; *p<0.05 for the effect of CYN154806; †p<0.05 for difference between Fh1βKO and wild-type pancreases at 1 mM glucose. *f*, Somatostatin secretion at 1 and 20 mM glucose in islets from non-diabetic (ND, n=32 donors) and type-2 diabetic donors (T2DM, n=7 donors). 1-way ANOVA with Tukey adjustment; ***p<0.001 *vs.* 1 mM glucose. ns (not significant), p=0.57. *g*, Glucagon secretion measured at 1 mM glucose in islets from ND (n=50 donors) and T2DM donors (n=12 donors). 1-way ANOVA with Tukey adjustment; *p<0.05, **p<0.01 *vs.* 1 mM; †p<0.05 *vs.* ND. *h*, Effect of the SSTR2 antagonist CYN154806 on glucagon secretion in islet preparations from three donors with T2D. Note that CYN154806 increases glucagon secretion in the two preparations with low glucagon secretion and that it had no effect on the preparation with high glucagon secretion. The shaded area and superimposed black line indicate glucagon secretion at 1 mM glucose in islets from non-diabetic donors (mean secretion ± S.E.M. in 41 preparations). *i*, Schematic summarising the stimulus-secretion coupling in δ-cell. Glucose uptake (via GLUT1 or 3) leads to stimulation of glucose metabolism (glycolysis and mitochondria) and

an increased cytoplasmic ATP/ADP ratio. This closes K_{ATP} channels in the plasma membrane, producing membrane depolarization and activation of voltage-gated Ca^{2+} channels (VGCC). Ca^{2+} influx associated with electrical activity triggers further increase in cytoplasmic Ca^{2+} ($[Ca^{2+}]_i$) by Ca^{2+}-induced Ca^{2+} release (CICR) in the sarco/endoplasmic reticulum (sER) by activation of ryanodine receptor 3 (RyR3) Ca^{2+} release channels. The resultant increase in $[Ca^{2+}]_i$ triggers somatostatin secretion. Inhibitors of the Ca^{2+} ATPase ('Ca^{2+} pump') of the sER (SERCA inhibitors; e.g. thapsigargin) inhibit somatostatin secretion by depleting sER of Ca^{2+}. Glucose also stimulates somatostatin secretion by elevation of intracellular Na^+ ($[Na^+]_i$) (possibly mediated by SGLTs) and thereby increases $[Ca^{2+}]_i$ via stimulation of *intra*cellular Na^+-Ca^{2+} exchange (NCLX) and thereby triggers CICR independently of electrical activity. Inhibition of the Na^+/K^+ ATPase (by low $[K^+]_o$) also increases $[Na^+]_i$ and triggers CICR.

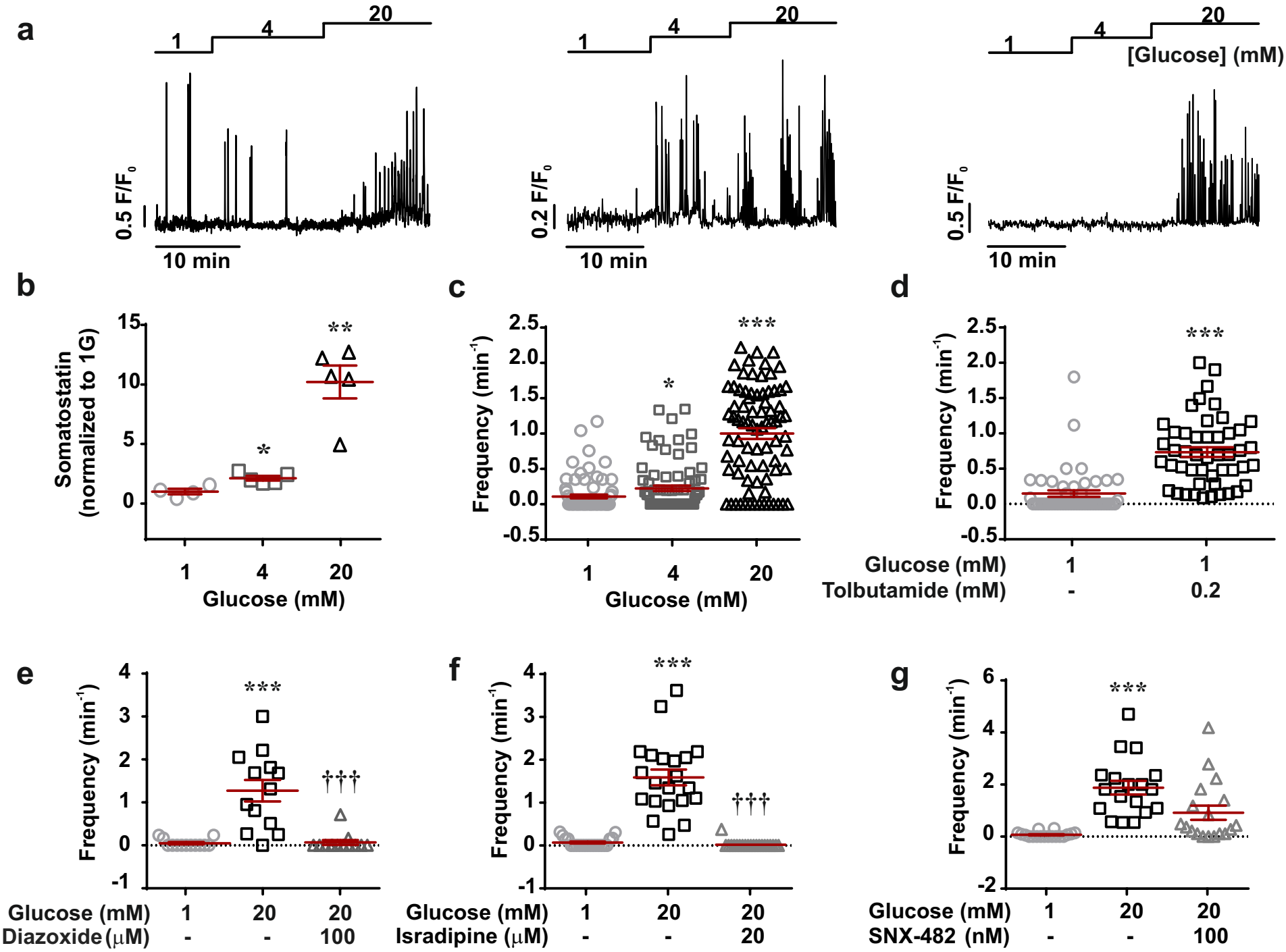

Vergari et al. Figure 1

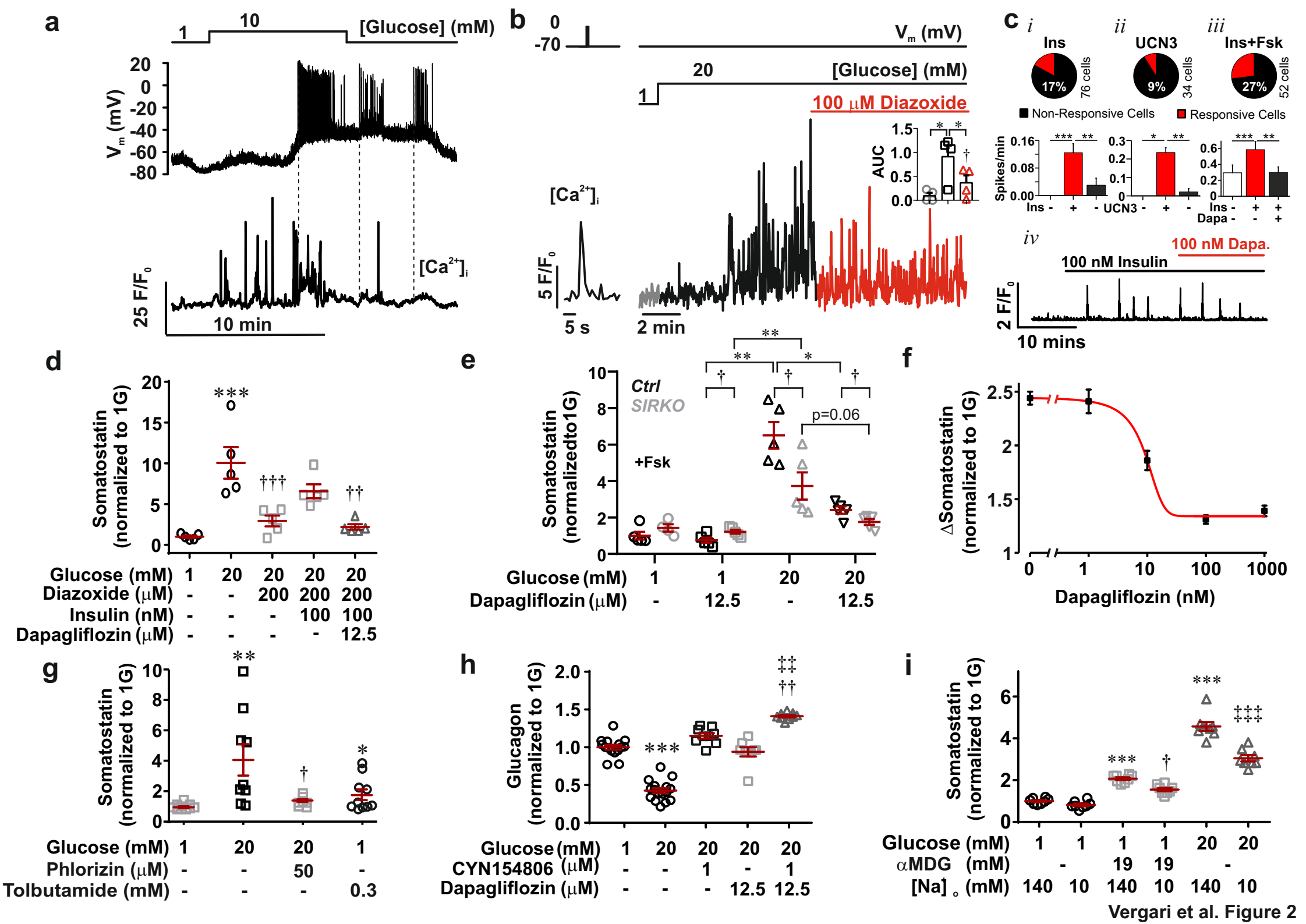

Vergari et al. Figure 2

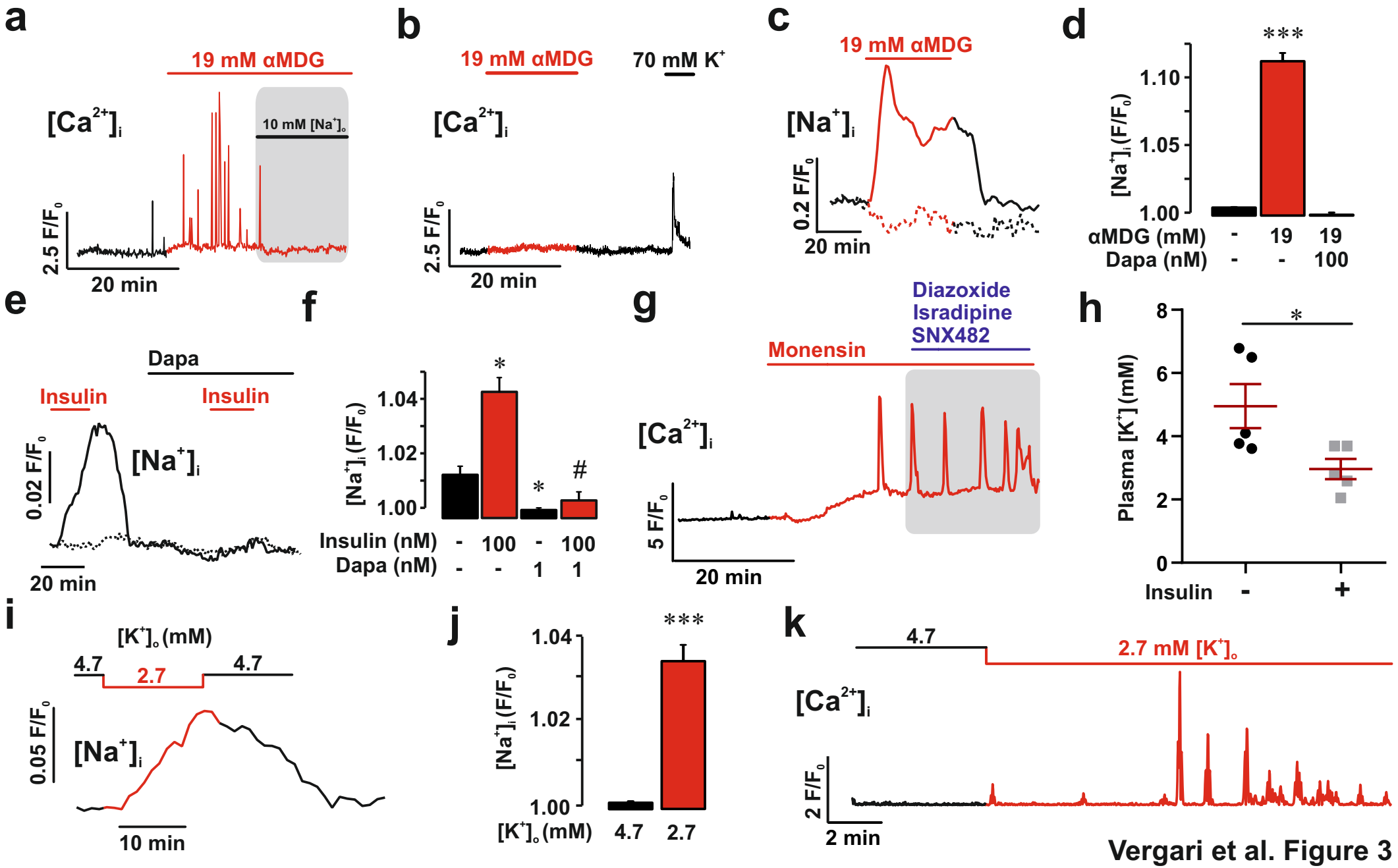

Vergari et al. Figure 3

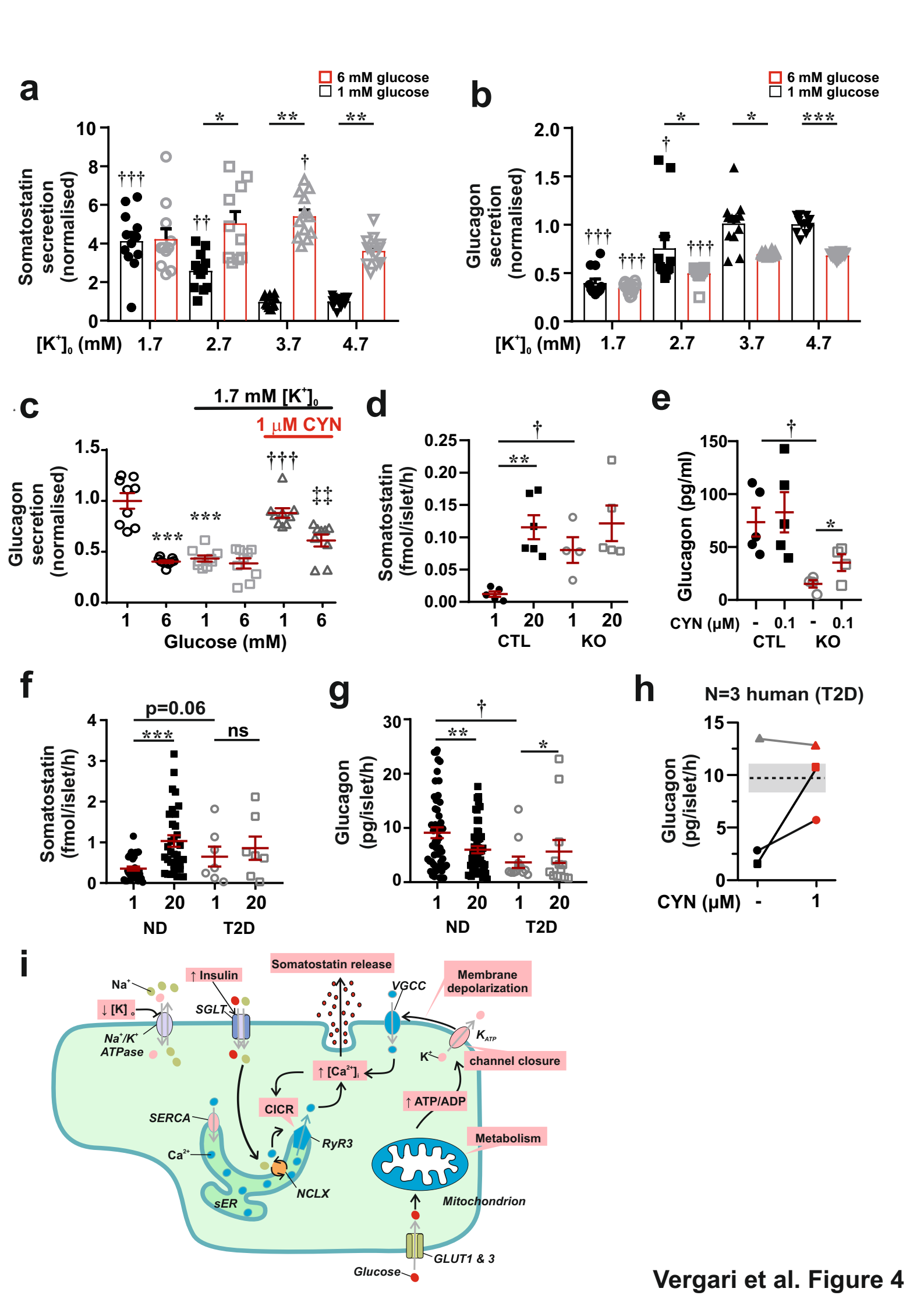

Vergari et al. Figure 4